© 2018. Published by The Company of Biologists Ltd | Journal of Experimental Biology (2018) 221, jeb177766. doi:10.1242/jeb.177766

RESEARCH ARTICLE

Analysis of vascular mechanical properties of the yellow anaconda reveals increased elasticity and distensibility of the pulmonary artery during digestion

Renato Filogonio[1,*], Tobias Wang[1] and Carl Christian Danielsen[2]

ABSTRACT

In animals with functional division of blood systemic and pulmonary pressures, such as mammals, birds, crocodilians and a few non-crocodilian reptiles, the vessel walls of systemic and pulmonary arteries are exquisitely adapted to endure different pressures during the cardiac cycle, systemic arteries being stronger and stiffer than pulmonary arteries. However, the typical non-crocodilian reptile heart possesses an undivided ventricle that provides similar systolic blood pressure to both circuits. This raises the question whether in these species the systemic and pulmonary mechanical vascular properties are similar. Snakes also display large organ plasticity and increased cardiac output in response to digestion, and we speculate how the vascular circuit would respond to this further stress. We addressed these questions by testing the mechanical vascular properties of the dorsal aorta and the right pulmonary artery of fasted and fed yellow anacondas, *Eunectes notaeus*, a snake without functional ventricular separation that also exhibits large metabolic and cardiovascular responses to digestion. Similar to previous studies, the dorsal aorta was thicker, stronger, stiffer and more elastic than the pulmonary artery. However, unlike any other species studied so far, the vascular distensibility (i.e. the relative volume change given a pressure change) was similar for the two circuits. Most striking, the pulmonary artery elasticity (i.e. its capacity to resume its original form after being stretched) and distensibility increased during digestion, which suggests that this circuit is remodeled to accommodate the larger stroke volume and enhance the Windkessel effect, thus providing a more constant blood perfusion during digestion.

KEY WORDS: Collagen, Dorsal aorta, Elastin, Postprandial period, Snakes, Sulfated glycosaminoglycans

INTRODUCTION

In mammals, the arteries in the systemic circulation typically experience much higher pressures than the pulmonary counterparts, which is reflected in both thicker and stronger walls (Greenfield and Patel, 1962; Greenfield and Griggs, 1963). This pattern also applies to some reptiles capable of ventricular pressure separation, such as the ball python, *Python regius* (Van Soldt et al., 2015). However, the heart of most reptiles is merely partially divided (Van Mierop and Kutsche, 1985; Jensen et al., 2014), such that the systemic and pulmonary arteries experience similar systolic pressure (Johansen, 1959; Burggren, 1977). Therefore, the unique python vasculature may not be a good representative of the typical reptilian arterial mechanics. Most likely, if the arterial walls from both circuits are well adapted to the same stress imposed during the cardiac cycle, their mechanical properties should be similar.

The extracellular matrix components of the arterial wall are responsible for many of its mechanical properties. Although collagen is the primary cause of arterial stiffness (Nichols et al., 2011), proteoglycans with sulfated glycosaminoglycans (sGAG) and hyaluronan also affect arterial stiffness (Gandley et al., 1997; Chai et al., 2005; Heegaard et al., 2007), whereas elasticity is provided by elastin (Sage and Gray, 1979; Nichols et al., 2011). Most collagen and elastin fibers are aligned in the circumferential direction in lamellar units, which is reflected in the vascular anisotropic (i.e. directionally dependent) mechanical properties (Wolinsky and Glagov, 1964, 1967; O'Connell et al., 2008), and sGAG are components in the ground substance of the extracellular matrix (Dingemans et al., 2000; Wagenseil and Mecham, 2009). In absolute terms, reptiles possess a stiffer systemic aorta than mammals (Gibbons and Shadwick, 1989), but values for stiffness normalized to *in vivo* blood pressure are astonishingly similar amongst vertebrates (Shadwick, 1999). It has been suggested that specific arterial composition and micro-structure confer the mechanical properties that enable arteries of different vertebrates to perform similarly at their normal *in vivo* pressures (Gibbons and Shadwick, 1989; Shadwick, 1999).

The snake vascular system experiences further mechanical stress during the postprandial period as a result of the concomitant rise in both heart rate and stroke volume (Secor et al., 2000; Secor and White, 2010; Zerbe et al., 2011; Enok et al., 2016). These adjustments are necessary to match the severalfold increase in metabolism over the course of numerous days following ingestion of large meals (Andrade et al., 1997; Andersen et al., 2005; Gavira and Andrade, 2013) along with the concomitant tissue growth (Secor and Diamond, 1998). Given their impressive organ plasticity, we speculate that the snake vasculature exhibits adaptive mechanical modifications to support this increased cardiovascular performance.

Arterial mechanics have been suggested to influence intracardiac blood shunt patterns in organisms without functional ventricular flow separation (Filogonio et al., 2017a,b; Hillman et al., 2014, 2017). In short, the equal systolic pressures in the systemic and pulmonary circuits would distend the more distensible vessels, thus delivering a greater portion of the stroke volume to that circuit (Hillman et al., 2014). Given the lack of studies concerning the typical reptilian cardiovascular circuit, in this study we compared the mechanical properties and collagen, elastin and sGAG content of the dorsal aorta and the pulmonary artery from the yellow anaconda, *Eunectes notaeus* Cope 1862 – a species without intraventricular

[1]Zoophysiology, Department of Bioscience, Aarhus University, 8000 Aarhus C, Denmark. [2]Department of Biomedicine, Aarhus University, 8000 Aarhus C, Denmark.

*Author for correspondence (renatofilogonio@gmail.com)

R.F., 0000-0002-5436-7102

Received 19 January 2018; Accepted 21 June 2018

Journal of Experimental Biology (2018) 221, jeb177766. doi:10.1242/jeb.177766

List of symbols and abbreviations

A	cross-sectional area
E	elastic modulus
F	load
F_{max}	maximum load
h	longitudinal height of the vessel segment
Δl	change in luminal perimeter
l_0	luminal perimeter at minimum load
MAP_{pul}	pulmonary mean arterial pressure
MAP_{sys}	systemic mean arterial pressure
P	pressure
P_{pul}	pulmonary systolic arterial pressure
P_{sys}	systemic systolic arterial pressure
r	luminal radius
sGAG	sulfated glycosaminoglycans
UC	unit collagen
V/V_0	relative volume change
ε	strain
ε_{max}	strain at maximum load
σ	stress

separation (Jensen et al., 2014). If distensibility is an important determinant of intracardiac blood shunts, systemic and pulmonary circuits should be largely different. We also analyzed fasted and digesting snakes to address possible vascular alterations due to the increased mechanical stress during the post-absorptive period.

MATERIALS AND METHODS

Experimental animals

Captive-bred yellow anacondas, *Eunectes notaeus* (n=14, mean±s.e.m. body mass 353±15 g), of undetermined sex, were acquired from commercial suppliers and maintained at the facilities of the Section of Zoophysiology, Aarhus University. There, they were kept inside 72 cm×40 cm×20 cm plastic boxes at room temperature (27–33°C), where they were fed with mice once a week and always had free access to water. Food was withheld for at least 2 weeks in the eight fasted snakes (343±18 g), whereas the six digesting snakes (366±26 g) were fed with mice (~10% of body mass) 2 days prior to harvesting the tissues. Data on standard dynamic action of snakes reveals large increases in metabolic rate (Andrade et al., 1997; Wang et al., 2002; Gavira and Andrade, 2013) and cardiac output (Zerbe et al., 2011; Enok et al., 2016) for similar meal sizes to those used in the present study. Animals were killed by isoflurane anesthesia followed by decapitation and pithing. Samples from the dorsal artery and the right pulmonary artery were collected and frozen until studied. All experiments were conducted in accordance with clause 53 of Danish experimental animal welfare regulations.

Histology

We analyzed histological sections from the dorsal aorta and the pulmonary artery from two fasted and two fed snakes. Dissected vessels for histology studies were mounted on plastic rods and fixed in 4% phosphate-buffered formaldehyde. Samples were then embedded in paraffin, sectioned in 4 µm transversal sections and stained with resorcin (Hart's solution), Sirius Red F3B, and Mayer's hematoxylin. Photographs were taken with an Olympus C-7070 WZ camera (Tokyo, Japan) mounted on a Leica DMRB microscope (Wetzlar, Germany), using both bright-field and circular polarization.

Tissue preparation and mounting

From each artery, four rings with 1 mm longitudinal height were cut and placed in a Tris/HCl buffer solution (50 mmol l^{-1}, pH 7.4). To determine cross-sectional area, we photographed rings mounted with minimal strain on tapered glass rods using a Nikon (Tokyo, Japan) microscope and analyzed the images with ImageJ v.1.50i. Ring specimens were pushed along the rod with a single-hair brush until the tapered glass rod filled the lumen of the rings (Van Soldt et al., 2015).

For mechanical testing, we used an in-house-built setup (described in detail by Van Soldt et al., 2015). Rings were thawed at room temperature before being mounted on parallel hooks (diameter: 0.35 or 0.18 mm; initial distance: 0.5 or 0.35 mm) submerged in the Tris/HCl buffer. The diameters of the hooks and the hook distances were low enough to allow ring specimens to be mounted unstrained. One hook was connected to a load cell with 1.8 N load capacity (Kistler-Morse DSC-6 transducer, DMT, Aarhus, Denmark), and the other was moved by a step motor (DM224i, API Motion, Amherst, NY, USA) at 0.1667 mm s^{-1}. Data on load and hook travel distance were continuously recorded by a data acquisition unit (Model 34970A, Hewlett Packard, Palo Alto, CA, USA) and from the motor drive, respectively. We

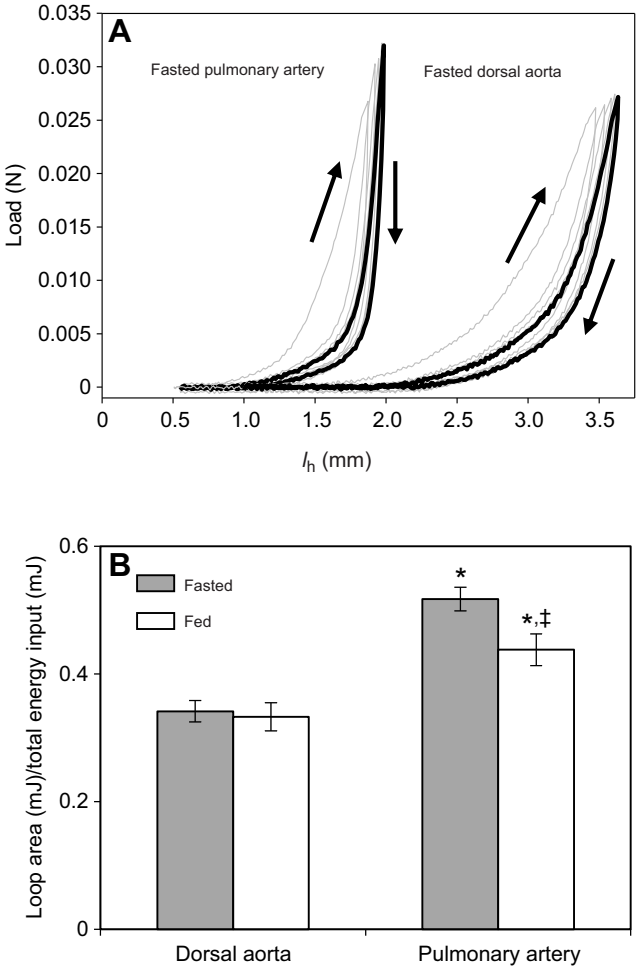

Fig. 1. Calculation of mechanical hysteresis (viscous damping). (A) Original recordings of loop cycles made by loading and unloading the vessels before testing to rupture. The arrows indicate the direction of the loop during loading and unloading. Data from the 5th cycle (in black) were used to calculate mechanical hysteresis. l_h, hook distance. (B) Mechanical hysteresis of the dorsal aorta and the pulmonary artery in fasted (n=8) and fed (n=6) animals. *Significant difference between the dorsal aorta and the pulmonary artery within the fasted or fed groups; ‡significant difference for the pulmonary artery between fasted and fed animals (two-way ANOVA; P<0.05; d.f.=27). Data are means±s.e.m.

Journal of Experimental Biology (2018) 221, jeb177766. doi:10.1242/jeb.177766

then subjected rings to five test cycles up to a maximum load of 25 mN to reach a steady state in the deformation and unloading response (Fig. 1A). Thereafter, we recorded load–deformation until rupture, and the ruptured rings were collected for hydroxyproline determination (Woessner, 1976; Danielsen and Andreassen, 1988). Collagen content was calculated as 7.46×hydroxyproline content (Neuman and Logan, 1950).

Determination of collagen, elastin and sGAG content

Fractions of elastin and collagen were calculated relative to dry defatted mass. Vessel samples were defatted with acetone and freeze-dried. Elastin content was determined by weighing after extraction of all other tissue components (Lansing et al., 1952). Aliquots of the extracts were used for sGAG and hydroxyproline determination. Collagen content was estimated as described above. For determination of total sGAG content, samples were treated with trypsin at 37°C overnight and centrifuged at 21,000 ***g*** for 5 min, following the procedures described by Barbosa et al. (2003). sGAG content is reported as μg mg^{-1} dry mass. Because of the small amount of tissue from the pulmonary artery, we could not determine elastin and sGAG content from each individual separately. To circumvent this problem, we analyzed three aliquots from each experimental group (fasted and fed). Each aliquot was composed of pooled samples from up to four individuals from that group, which allowed us to attain the minimum dry mass reading necessary to perform accurate measurements.

Calculation of mechanical properties

Part of the force absorbed by the vessel during stretching is lost during unloading through viscous damping, resulting in the hysteresis loops depicted in Fig. 1A. The ratio between the energy lost (loop area) and total energy input (area under the loading curve) is called mechanical

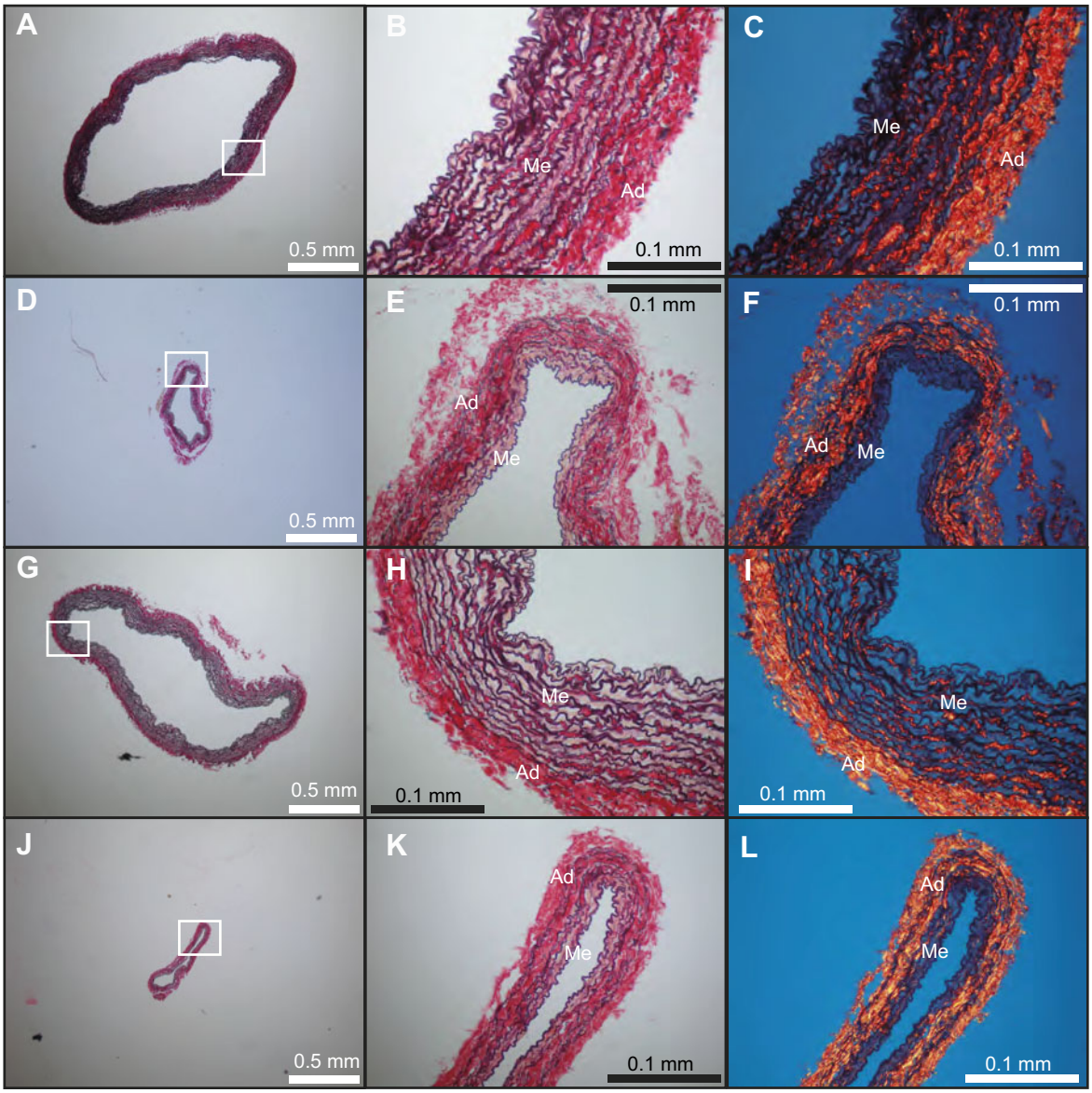

Fig. 2. Histological cross-sectional cuts from the dorsal aorta (A–C,G–I) and the pulmonary artery (D–F,J–L) of *Eunectes notaeus*. (A–F) Photos from fasted animals; (G–L) photos from fed animals. In the bright-field photos (left and middle column) collagen appears as red, smooth muscle cells as yellow/light pink and elastin as dark purple. In the photos with circular polarization (right column), collagen appears as red, orange or yellow, and elastin as dark blue. Panels in the left column are represented at a higher magnification in the middle column. Ad, tunica adventitia; Me, tunica media.

Journal of Experimental Biology (2018) 221, jeb177766. doi:10.1242/jeb.177766

hysteresis and indicates the relative importance of viscosity to the arterial mechanical response, such that higher mechanical hysteresis indicates lower elasticity (Shadwick, 1992). We used the areas from the 5th loop (Fig. 1A) to calculate mechanical hysteresis from the dorsal aorta and the pulmonary artery under fasted and fed conditions.

Maximum load (F_{max}) and strain at F_{max} (ε_{max}) were derived from load–strain curves. Strain ($\varepsilon=\Delta l/l_0$) is the change in luminal perimeter (Δl) relative to luminal perimeter (l_0) at a minimum load (0.2 mN). Stress (σ) was calculated as load (F) per cross-sectional area (A; $\sigma=F/A$). We also normalized F_{max} to unit collagen (UC: mg of collagen divided by the segment's l_0) to assess the mechanical quality of the collagen (N mg^{-1} mm).

Distensibility curves were drawn plotting calculated pressure change {$P=2\pi F/[l_0(1+\varepsilon)h]$, where h is longitudinal height of the segment; Van Soldt et al., 2015} against relative volume change [$V/V_0=(1+\varepsilon)^2$]. Elastic modulus (E) was derived from the slope of the stress–strain curves ($E=\Delta\sigma/\Delta\varepsilon$) and plotted against either pressure or pressure normalized to specific mean arterial pressure (MAP_{pul}=3.41 kPa, MAP_{sys}=5.15 kPa for pulmonary and systemic, respectively; P. B. M. Pedersen, A. Findsen, J. L. Andersen, K. Hansen and T.W., unpublished data). Stiffness–strain curves were derived from the slope of the load–strain curves. Stiffness and strain corresponding to pressures of 1.5, 5 and 11 kPa (equivalent to minimum diastolic pulmonary pressure, mean systemic pressure and systolic pressure during adrenergic stimulation, respectively; P. Pedersen et al., unpublished data) were estimated by finding the combination of load and strain fulfilling the equation for P [$P=F/(r\times h)$; where r is the luminal radius: $r=l/2\pi$; Van Soldt et al., 2015].

Statistical analysis

The mechanical properties and dimensions for each snake were represented by the average of four ring specimens. To test the effects of artery type (dorsal aorta or pulmonary artery) and digestive state (fasted or fed) on mechanical vascular properties, we used two-way ANOVA followed by Tukey's *post hoc* test ($P<0.05$). Data met assumptions of normality and homoscedasticity, and tests were performed with SigmaPlot v.11 (Systat Software Inc., 2008). Data are presented as means±s.e.m.

RESULTS

Histology

Histological sections revealed no differences between fasting and digesting snakes for either dorsal aorta or pulmonary artery. The transverse sections showed that the dorsal aorta (Fig. 2A–C,G–I) is thicker than the pulmonary artery (Fig. 2D–F,J–L). The dorsal aorta wall consisted mainly of the tunica media, where we observed elastin arranged in wavy and circumferential lamellae (Fig. 2B,H), and smooth muscle cells between the lamellar structures (light pink structures in Fig. 2B,H). The relative size of the tunica media in the pulmonary artery, with only a few elastic lamellae, was smaller than in the dorsal aorta (Fig. 2E,K). The polarized images indicate some collagen content interspaced between the lamellar structures of elastin at the tunica media, but it is mostly concentrated at the tunica adventitia (Fig. 2C,F,I,L). The relative size of the adventitia compared with the wall thickness was greater in the pulmonary artery (Fig. 2F,L) than in the dorsal aorta (Fig. 2C,I).

Arterial wall composition and dimensions

The pulmonary artery presented a consistently higher collagen (~56%) and lower elastin content (~60%) than the dorsal aorta, whereas the sGAG content was similar in the two arteries (Table 1). Diameter and cross-sectional area of the dorsal aorta were both higher than those of the pulmonary artery (Table 2). Interestingly, the two arteries presented similar values of collagen content per mm of luminal perimeter (UC; Table 2). Digestive state did not affect any of the variables analyzed for arterial composition (Table 1) or dimension (Table 2).

Table 1. Collagen, elastin and sulfated glycosaminoglycan (sGAG) content relative to dry mass of dorsal aorta and pulmonary artery in fasted and fed snakes

Treatment	Collagen (%)	Elastin (%)	sGAG (μg mg^{-1})
Dorsal aorta			
Fasted (*n*=8)	27.9±0.7	27.5±1.2	3.4±0.2
Fed (*n*=6)	24.7±0.7	25.9±1.1	3.2±0.3
Total (*n*=14)	26.5±0.7	26.8±0.9	3.3±0.2
Pulmonary artery			
Fasted (*n*=3)	41.8±1.4	10.8±0.4	3.4±0.4
Fed (*n*=3)	39.6±1.4	9.3±0.4	2.8±0.5
Total (*n*=6)	40.7±1.0	10.1±0.4	3.1±0.3

Mechanical properties

Cycling tests showed that the dorsal aorta was more elastic than the pulmonary artery. Fed snakes presented a more elastic pulmonary artery than fasted snakes (Fig. 1B). The dorsal aorta also supported higher maximum loads (Fig. 3A), even though the two arteries could resist similar wall stresses (Fig. 3B). Normalization of F_{max} to unit collagen demonstrated that the collagen from the dorsal aorta resists larger loads than the collagen in the pulmonary artery (Table 2). The dorsal aorta was stiffer at all physiologically relevant pressures (Fig. 4A). The pulmonary artery for fed snakes presented a higher stiffness than the pulmonary artery of fasted snakes at 11 kPa (Fig. 4A). For all tested group treatments, the stiffness–strain curve started to increase at low strain values, followed by a reduced slope, which increased again at higher strain, thus depicting a 'shoulder' shape at the beginning of the curve (Fig. 3C). Interestingly, the stiffness and strain values for pressures as high as 11 kPa fell within the limits of this 'shoulder' shape (Fig. 3C), thus indicating that arterial walls routinely work at very low pressure-induced stiffness, stress and load.

We found no differences in strain at F_{max} for any of the tested groups (Fig. 3A). However, we observed significant differences at the physiologically relevant pressure range. Strain for the dorsal aorta was the same for the fasted and fed snakes at all three pressures estimated (Fig. 4B). The values were higher than those for the pulmonary artery of fasted snakes at 1.5 kPa, but similar for higher

Table 2. Diameter, cross-sectional area, unit collagen (UC) and maximum load (F_{max}) normalized to UC, for dorsal aorta and pulmonary artery in fasted and fed snakes

Treatment	Diameter (mm)	Cross-sectional area (mm^2)	UC (mg mm^{-1})	F_{max} normalized to UC (N mg^{-1} mm)
Dorsal aorta				
Fasted (*n*=8)	1.57±0.04	0.18±0.01	0.0089±0.0005	42.62±1.67
Fed (*n*=6)	1.63±0.06	0.19±0.01	0.0093±0.0005	43.85±3.21
Pulmonary artery				
Fasted (*n*=8)	0.65±0.03*	0.09±0.02*	0.0089±0.0021	27.51±4.28*
Fed (*n*=6)	0.72±0.06*	0.07±0.01*	0.0064±0.0010	30.28±5.25*

*Significant difference between pulmonary artery and dorsal aorta for fasted and fed snakes, respectively (two-way ANOVA; $P<0.05$; d.f.=27). Data are means±s.e.m.

Journal of Experimental Biology (2018) 221, jeb177766. doi:10.1242/jeb.177766

pressures (Fig. 4B). The pulmonary artery of fed snakes, however, consistently presented higher strain values than those of fasted animals at all pressures tested (Fig. 4B). These values were equal to those for the dorsal aorta at 1.5 kPa but higher at 5 and 11 kPa (Fig. 4B). The relative volume change–pressure curves clearly corroborate these results and demonstrate that distensibility of the

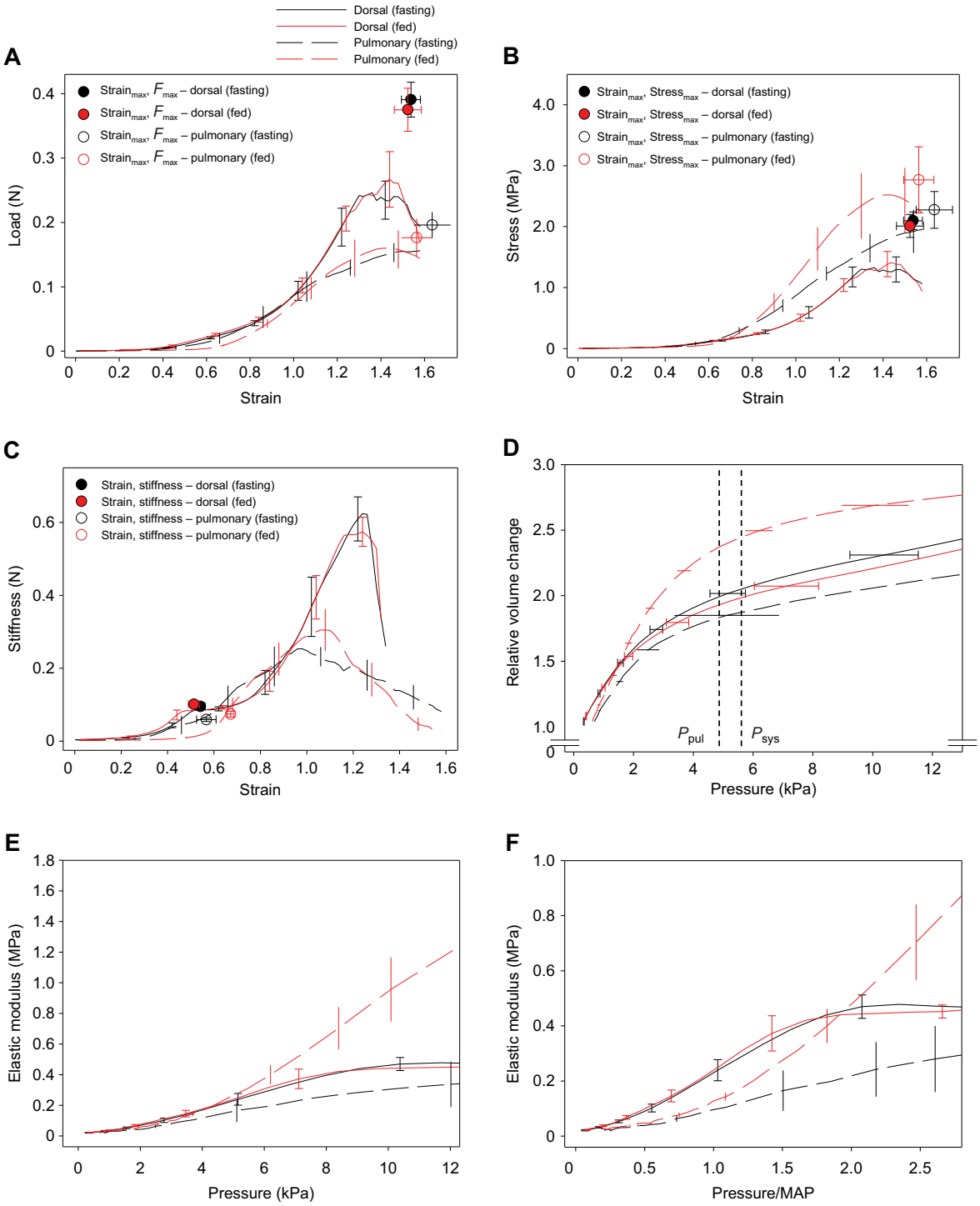

Fig. 3. Mechanical curves for dorsal aorta (solid lines) and pulmonary artery (dashed lines) for fasted (black lines) and fed (red lines) *E. notaeus*. (A) Load–strain curves. Symbols indicate maximum strain at maximum load for dorsal aorta (filled circles) and pulmonary artery (open circles) in fasted (black) and fed (red) snakes. (B) Stress–strain curves. Symbols indicate maximum strain at maximum stress for dorsal aorta (filled circles) and pulmonary artery (open circles) in fasted (black) and fed (red) snakes. (C) Stiffness–strain curves. Symbols indicate the stiffness–strain relationship corresponding to a blood pressure of 11 kPa for dorsal aorta (filled circles) and pulmonary artery (open circles) in fasted (black) and fed (red) snakes. (D) Distensibility curves, with vertical broken lines indicating the systolic arterial pressure for the pulmonary circuit (P_{pul}) and the systemic circuit (P_{sys}) of anesthetized *E. notaeus*. (E) Elastic modulus–pressure relationship. (F) Elastic modulus–pressure normalized by mean pulmonary arterial pressure (MAP, 3.41 kPa) or the systemic mean arterial pressure (5.15 kPa). Blood pressure values were obtained from P. B. M. Pedersen, A. Findsen, J. L. Andersen, K. Hansen and T.W. (unpublished data). Lines represent mean values and error bars are s.e.m.

Journal of Experimental Biology (2018) 221, jeb177766. doi:10.1242/jeb.177766

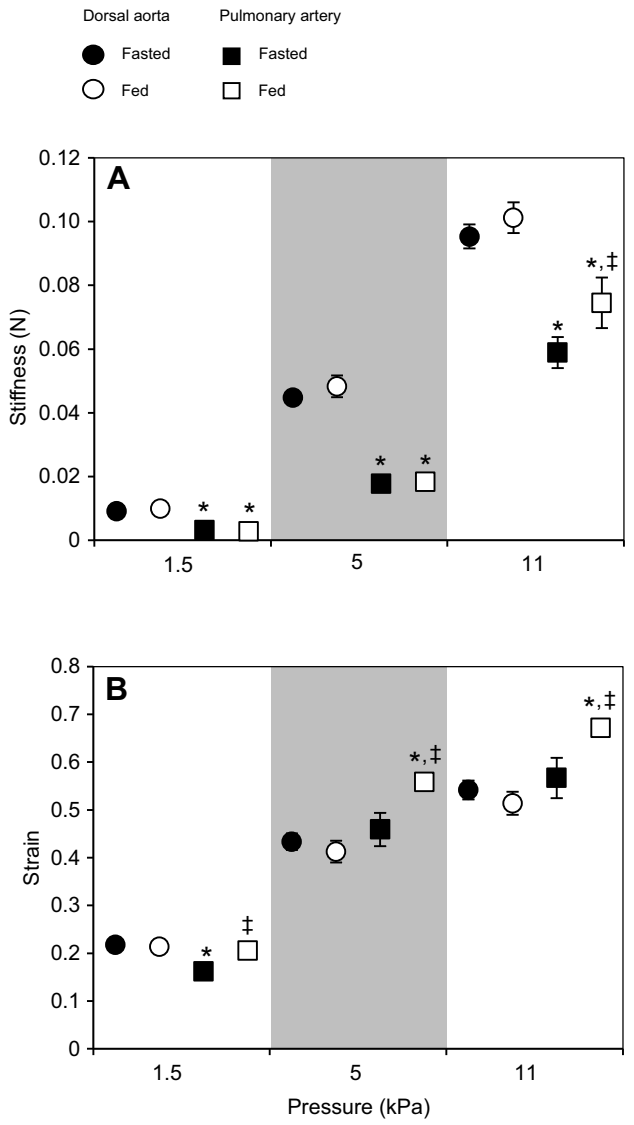

Fig. 4. Stiffness and strain at different blood pressures (1.5, 5 and 11 kPa). (A) Stiffness and (B) strain (normalized values). Filled symbols indicate fasted snakes (n=8) and open symbols indicate fed snakes (n=6). *Significant difference between dorsal aorta (circles) and pulmonary arteries (squares). ‡Significant difference for the pulmonary artery between fasted and fed animals (two-way ANOVA; P<0.05; d.f.=27). Data are means±s.e.m.

dorsal aorta and pulmonary artery are similar for fasted animals, with a notable increase of pulmonary artery distensibility for fed animals (Fig. 3D).

All vessels exhibited a similar elastic modulus until around 6 kPa (Fig. 3E). At higher pressures, the elastic modulus from the pulmonary artery from fed snakes started to increase more than that of the other arteries (Fig. 3E). Elastic modulus for normalized pressures to specific MAP shows differences between the dorsal aorta and the pulmonary artery, and indicates that the pulmonary artery displays a lower elastic modulus at normal pressure conditions (Fig. 3F). Elastic modulus of the pulmonary artery of fed animals resembled that of the dorsal aorta when blood pressures doubled (Fig. 3F).

DISCUSSION

Many of the mechanical properties reported in the present study for *E. notaeus*, a species with the typical reptilian undivided heart, contrast with the findings from *P. regius* (Van Soldt et al., 2015), a species with intraventricular pressure separation (Wang et al., 2003). In *P. regius*, the dorsal aorta and the pulmonary arteries differ in ε_{max}, distensibility, E and UC values (Van Soldt et al., 2015), whereas in fasted *E. notaeus* those parameters are similar (Table 3). Thus, *E. notaeus* is the first example of a vertebrate displaying equal arterial systemic and pulmonary distensibilities. Additionally, when E was normalized to the corresponding *in vivo* MAP (Fig. 3F), E values were well below those reported for any other species (Gibbons and Shadwick, 1989; Shadwick, 1999; Van Soldt et al., 2015), which suggests structural differences in the arterial walls of the yellow anaconda. Unlike *P. regius*, *E. notaeus* does not exhibit intraventricular functional separation and those results corroborate the hypothesis that its vascular circuit is well adapted to support similar systolic pressures during the cardiac cycle, in contrast to what was demonstrated for *P. regius* (Van Soldt et al., 2015).

Arterial collagen and elastin content of *E. notaeus* were remarkably similar to that of *P. regius* (Van Soldt et al., 2015). The diameter of the right pulmonary artery of *P. regius* was about three times larger than that of *E. notaus* (Table 3), which explains its lower UC values. However, the lower mechanical quality of the collagen (i.e. lower capability to endure higher loads) in the pulmonary artery of *E. notaeus* versus *P. regius* (Van Soldt et al., 2015; Table 3) indicates differences in collagen isoforms, cross-linking, fiber orientation or interaction between extracellular matrix components (Dingemans et al., 2000; MacDonald et al., 2000; Humphrey, 2008; Wagenseil and Mecham, 2009).

Although there are no reports on the quantification of arterial sGAG in reptiles, the values found for *E. notaeus* were lower than those for the human aorta (~30 µg mg^{-1}: Stevens et al., 1976; ~8 µg mg^{-1}: Cardoso and Mourão, 1994) and the pulmonary artery (~7 µg mg^{-1}: Cardoso and Mourão, 1994), albeit comparable to those for the dog aorta (~3 µg mg^{-1}: Sirek et al., 1977). Although sGAG content may influence arterial stiffness in rats (Gandley et al., 1997), the similar values of sGAG content in the dorsal aorta and the pulmonary artery in *E. notaeus* cannot explain the higher stiffness of the dorsal aorta. Thus, these differences might result from the dissimilar arterial wall thickness or the influence of other components.

Table 3. Mechanical properties and dimensions of the dorsal aorta and the right pulmonary artery of the ball python, *Python regius*, compared with those of fasted yellow anaconda, *Eunectes notaeus* (present study)

	Python regius	
Parameters	Dorsal aorta	Right pulmonary artery
ε_{max}	1.35 (~)	1.05 (<)
Distensibility*	Small initial volume change	Large initial volume change
E (MPa) versus P (kPa)*	Small E change	Large E change
Diameter (mm)‡	2.2 (>)	2.2 (>)
UC (mg mm^{-1})	0.010 (~)	0.004 (<)
F_{max} normalized for UC (N mg^{-1} mm)	40 (~)	60 (>)

Python regius data are from Van Soldt et al. (2015).
Parameters are strain at maximum load (ε_{max}), distensibility, elastic modulus (E; MPa) versus pressure (P; kPa), diameter (mm), unit collagen (UC; mg mm^{-1}), maximum load (F_{max}) normalized to UC (N mg^{-1} mm). Symbols in parentheses are as follows: ~, similar; <, lower; and >, higher.
*Distensibility and E from dorsal aorta and pulmonary artery in fasted *E. notaeus* were similar.
‡The dorsal aorta from *E. notaeus* had a bigger diameter than the pulmonary artery.

It has been suggested that vascular mechanical properties may be of particular importance to determine cardiac shunt patterns in organisms with an undivided ventricle, such as amphibians and reptiles (Hillman et al., 2014). In fasting snakes, we found similar distensibilities of the major conductance arteries in the two circuits. Thus, an increase in systolic pressures alone would not justify changes in cardiac shunts such as those observed during activity (Krosniunas and Hicks, 2003; Filogonio et al., 2016). This agrees with the meta-analysis by Filogonio et al. (2017a), where there was no general relationship between shunt patterns and increase in cardiac output, suggesting that mechanical properties, such as passive distensibility, are probably of minor importance in determining cardiac shunt patterns in reptiles.

Interestingly, both elastic efficiency and distensibility of the pulmonary artery increased during digestion. It might seem counter-intuitive that changes in cardiac output lead to adjustment of various components of the vessel wall, rather than a faster regulatory response driven by the plethora of neural, local and humoral factors known to influence vessel tone of snakes and other vertebrates (Gunnes et al., 1983, 1985; Sowden et al., 2007; Enok et al., 2012). There is a lack of information, however, on how the pulmonary vasculature reacts to those effectors, particularly in non-mammalian vertebrates. The only study that measured chronic changes of pulmonary blood flow in a conscious reptile after feeding showed that the common snapping turtle, *Chelydra serpentina*, reduces the left to right cardiac shunt (i.e. systemic bypass of the blood flow), indicating that systemic resistance decreases more than pulmonary resistance (Wearing et al., 2017). This hints at the possibility that smooth muscle regulation during the postprandial period plays a more important role in regulating the systemic vasculature, where we observed no changes in mechanical properties of the dorsal aorta, than in the pulmonary arteries.

Boid snakes, such as the yellow anaconda, are infrequent feeders and may ingest very large meals (e.g. ∼30% of their own body mass; Wang et al., 2001), compressing blood vessels peripheral to the stomach and possibly altering blood circulation. Interestingly, mean arterial pressures are unaffected during digestion (Wang et al., 2001; Enok et al., 2012), even during large increases of cardiac output (Enok et al., 2016). Furthermore, the vascularized region of snakes' lungs is located anterior to the stomach (Chiodini et al., 1982; Isaza et al., 1993), and the compression of the lungs is unlikely to impair pulmonary blood flow upon meal ingestion. Hence, altered elasticity and distensibility are probably not a response to this stress.

However, snakes typically experience visceral organ volume growth of severalfold during the postprandial period (Secor and Diamond, 1998; Starck and Beese, 2001, 2002) – the heart being an exception (Hansen et al., 2013; Slay et al., 2014; Henriksen et al., 2015) – followed by large increases in cardiac output through heart rate and stroke volume modulation (Secor et al., 2000; Secor and White, 2010; Zerbe et al., 2011; Enok et al., 2016). As we did not observe any change in the arterial composition, the increased distensibility of the pulmonary artery is probably due to a structural modification to accommodate this higher cardiac output, while the increased elasticity probably improves the Windkessel effect, thus providing a proper blood perfusion for the lungs during digestion.

Conclusion

The pulmonary vasculature has a certain level of plasticity, possibly to accommodate the larger stroke volume during the postprandial period (Zerbe et al., 2011; Enok et al., 2016). Also, although the arterial composition of *E. notaeus* is very similar to that of *P. regius*, many mechanical properties are dramatically different between the two species (Table 3). Thus, while the peculiar cardiovascular design of the ball python withstands very different systemic and pulmonary blood pressures, the systemic and pulmonary vasculature of *E. notaeus*, a species without intraventricular pressure separation, are exquisitely adapted to sustain equal systolic pressures during the cardiac cycle.

Acknowledgements

We thank Heidi M. Jensen for taking care of the snakes, Jytte Utoft for help during the preparation of histological sections, and Benjamin Van Soldt for valuable discussions on arterial mechanics.

Competing interests

The authors declare no competing or financial interests.

Author contributions

Conceptualization: R.F., T.W., C.C.D.; Methodology: R.F., T.W., C.C.D.; Software: C.C.D.; Validation: R.F., C.C.D.; Formal analysis: R.F., C.C.D.; Investigation: R.F., C.C.D.; Resources: T.W., C.C.D.; Data curation: C.C.D.; Writing - original draft: R.F.; Writing - review & editing: R.F., T.W., C.C.D.; Visualization: T.W.; Supervision: T.W., C.C.D.; Project administration: T.W., C.C.D.; Funding acquisition: R.F., T.W., C.C.D.

Funding

R.F. received a scholarship from Coordenação de Aperfeiçoamento de Pessoal de Nível Superior (CAPES) through the Science without Borders program (process no. 8938-13-0); T.W. had financial support from Natur og Univers, Det Frie Forskningsråd (FNU).

References

Andersen, J. B., Rourke, B. C., Caiozzo, V. J., Bennett, A. F. and Hicks, J. W. (2005). Postprandial cardiac hypertrophy in pythons. *Nature* **434**, 37-38.

Andrade, D. V., Cruz-Neto, A. P. and Abe, A. S. (1997). Meal size and specific dynamic action in the rattlesnake *Crotalus durissus* (Serpentes: Viperidae). *Herpetologica* **53**, 485-493.

Barbosa, I., Garcia, S., Barbier-Chassefière, V., Caruelle, J. P., Martelly, I. and Papy-García, D. (2003). Improved and simple micro assay for sulfated glycosaminoglycans quantification in biological extracts and its use in skin and muscle tissue studies. *Glycobiology* **13**, 647-653.

Burggren, W. W. (1977). The pulmonary circulation of the chelonian reptile: morphology, haemodynamics and pharmacology. *J. Comp. Physiol. B* **116**, 303-323.

Cardoso, L. E. and Mourão, P. A. (1994). Glycosaminoglycan fractions from human arteries presenting diverse susceptibilities to atherosclerosis have different binding affinities to plasma LDL. *Arterioscler. Thromb. Vasc. Biol.* **14**, 115-124.

Chai, S., Chai, Q., Danielsen, C. C., Hjorth, P., Nyengaard, J. R., Ledet, T., Yamaguchi, Y., Rasmussen, L. M. and Wogensen, L. (2005). Overexpression of hyaluronan in the tunica media promotes the development of atherosclerosis. *Circ. Res.* **96**, 583-591.

Chiodini, R. J., Sundberg, J. P. and Czikowsky, J. A. (1982). Gross anatomy of snakes. *Vet. Med. Small Anim. Clin.* **77**, 413-419.

Danielsen, C. C. and Andreassen, T. T. (1988). Mechanical properties of rat tail tendon in relation to proximal-distal sampling position and age. *J. Biomech.* **21**, 207-212.

Dingemans, K. P., Teeling, P., Lagendijk, J. H. and Becker, A. E. (2000). Extracellular matrix of the human aortic media: an ultrastructural histochemical and immunohistochemical study of the adult aortic media. *Anat. Rec.* **258**, 1-14.

Enok, S., Simonsen, L. S., Pedersen, S. V., Wang, T. and Skovgaard, N. (2012). Humoral regulation of heart rate during digestion in pythons (*Python molurus* and *Python regius*). *Am. J. Physiol. Regul. Integr. Comp. Physiol.* **302**, R1176-R1183.

Enok, S., Leite, G. S. P. C., Leite, C. A. C., Gesser, H., Hedrick, M. S. and Wang, T. (2016). Improved cardiac filling facilitates the postprandial elevation of stroke volume in *Python regius*. *J. Exp. Biol.* **219**, 3009-3018.

Filogonio, R., Wang, T., Taylor, E. W., Abe, A. S. and Leite, C. A. C. (2016). Vagal tone regulates cardiac shunts during activity and at low temperatures in the South American rattlesnake, *Crotalus durissus*. *J. Comp. Physiol. B* **186**, 1059-1066.

Filogonio, R., Leite, C. A. C. and Wang, T. (2017a). Vascular distensibilities have minor effects on intracardiac shunt patterns in reptiles. *Zoology* **122**, 46-51.

Filogonio, R., Leite, C. A. C. Wang, T. (2017b). Reply to the commentary by Hillman et al. on: "Vascular distensibilities have minor effects on intracardiac shunt patterns in reptiles" by Filogonio et al. (2017). *Zoology* **122**, 55-57.

Gandley, R. E., McLaughlin, M. K., Koob, T. J., Little, S. A. and McGuffee, L. J. (1997). Contribution of chondroitin-dermatan sulfate-containing proteoglycans to

the function of rat mesenteric arteries. *Am. J. Physiol. Heart. Circ. Physiol.* **42**, H952-H960.
Gavira, R. S. B. and Andrade, D. V. (2013). Meal size effects on the postprandial metabolic response of *Bothrops alternatus* (Serpentes: Viperidae). *Zoologia* **30**, 291-295.
Gibbons, C. A. and Shadwick, R. E. (1989). Functional similarities in the mechanical design of the aorta in lower vertebrates and mammals. *Experientia* **45**, 1083-1088.
Greenfield, J. C. and Griggs, D. M. (1963). Relation between pressure and diameter in main pulmonary artery of man. *J. Appl. Physiol.* **18**, 557-559.
Greenfield, J. C. and Patel, D. J. (1962). Relation between pressure and diameter in the ascending aorta. *Circ. Res.* **10**, 778-781.
Gunnes, P., Waldum, H. L., Rasmussen, K., Østensen, H. and Burhol, P. G. (1983). Cardiovascular effects of secretin infusion in man. *Scand. J. Clin. Lab. Invest.* **43**, 637-642.
Gunnes, P., Smiseth, O. A., Lygren, I. and Jorde, R. (1985). Effects of secretin infusion on myocardial performance and metabolism in the dog. *J. Cardiovasc. Pharmacol.* **7**, 1183-1187.
Hansen, K., Pedersen, P. B. M., Pedersen, M. and Wang, T. (2013). Magnetic resonance imaging volumetry for noninvasive measures of phenotypic flexibility during digestion in Burmese Pythons. *Physiol. Biochem. Zool.* **86**, 149-158.
Heegaard, A.-M., Corsi, A., Danielsen, C. C., Nielsen, K. L., Jorgensen, H. L., Riminucci, M., Young, M. F. and Bianco, P. (2007). Biglycan deficiency causes spontaneous aortic dissection and rupture in mice. *Circulation* **115**, 2731-2738.
Henriksen, P. S., Enok, S., Overgaard, J. and Wang, T. (2015). Food composition influences metabolism, heart rate and organ growth during digestion in *Python regius*. *Comp. Biochem. Physiol. A* **183**, 36-44.
Hillman, S. S., Hedrick, M. S. and Kohl, Z. F. (2014). Net cardiac shunts in anuran amphibians: physiology or physics? *J. Exp. Biol.* **217**, 2844-2847.
Hillman, S. S., Hedrick, M. S. and Kohl, Z. F. (2017). Commentary on: "Distensibilities have minor importance in determining cardiac shunt patterns in reptiles" by Filogonio et al. (2017). *Zoology* **122**, 52-54.
Humphrey, J. D. (2008). Mechanisms of arterial remodeling in hypertension: coupled roles of wall shear stress and intramural stress. *Hypertension* **52**, 195-200.
Isaza, R., Ackerman, N. and Jacobson, E. R. (1993). Ultrasound imaging of the coelomic structures in the boa constrictor (*Boa constrictor*). *Vet. Radiol. Ultrasound* **34**, 445-450.
Jensen, B., Moorman, A. F. M. and Wang, T. (2014). Structure and function of the hearts of lizards and snakes. *Biol. Rev.* **89**, 302-336.
Johansen, K. (1959). Circulation in the three-chambered snake heart. *Circ. Res.* **7**, 828-832.
Krosniunas, E. H. and Hicks, J. W. (2003). Cardiac output and shunt during voluntary activity at different temperatures in the turtle, *Trachemys scripta*. *Physiol. Biochem. Zool.* **76**, 679-694.
Lansing, A. I., Rosenthal, T. B., Alex, M. and Dempsey, E. W. (1952). The structure and chemical characterization of elastic fibers as revealed by elastase and by electron microscopy. *Anat. Rec.* **115**, 555-575.
MacDonald, D. J., Finlay, H. M. and Canham, P. B. (2000). Directional wall strength in saccular brain aneurysms from polarized light microscopy. *Ann. Biomed. Eng.* **28**, 533-542.
Neuman, R. E. and Logan, M. A. (1950). The determination of collagen and elastin in tissues. *J. Biol. Chem.* **186**, 549-556.
Nichols, W. W., O'Rourke, M. F. and Vlachopoulos, C. (2011). *McDonald's Blood Flow In Arteries: Theoretical, Experimental And Clinical Principles*, 6th edn. Boca Raton, FL: CRC Press.
O'Connell, M. K., Murthy, S., Phan, S., Xu, C., Buchanan, J., Spilker, R., Dalman, R. L., Zarins, C. K., Denk, W. and Taylor, C. A. (2008). The three-dimensional micro- and nanostructure of the aortic medial lamellar unit measured using 3D confocal and electron microscopy imaging. *Mat. Biol.* **27**, 171-181.
Sage, H. and Gray, W. R. (1979). Studies on the evolution of elastin–I Phylogenetic distribution. *Comp Biochem Physiol B* **64**, 313-327.
Secor, S. M. and Diamond, J. (1998). A vertebrate model of extreme physiological regulation. *Nature* **395**, 659-662.
Secor, S. M. and White, S. E. (2010). Prioritizing blood flow: cardiovascular performance in response to the competing demands of locomotion and digestion for the Burmese python, *Python molurus*. *J. Exp. Biol.* **213**, 78-88.
Secor, S. M., Hicks, J. W. and Bennett, A. F. (2000). Ventilatory and cardiovascular responses of a python (*Python molurus*) to exercise and digestion. *J. Exp. Biol.* **203**, 2447-2454.
Shadwick, R. E. (1992). Soft composites. In *Biomechanics—Materials: A Practical Approach* (ed. J. F. V. Vincent), pp. 133-164. Oxford: Oxford University Press.
Shadwick, R. E. (1999). Mechanical design in arteries. *J. Exp. Biol.* **202**, 3305-3313.
Sirek, O. V., Sirek, A. and Fikar, K. (1977). The effect of sex hormones on glycosaminoglycan content of canine aorta and coronary arteries. *Artherosclerosis* **27**, 227-233.
Slay, C. E., Enok, S., Hicks, J. W. and Wang, T. (2014). Reduction of blood oxygen levels enhances postprandial cardiac hypertrophy in Burmese python (*Python bivittatus*). *J. Exp. Biol.* **217**, 1784-1789.
Sowden, G. L., Drucker, D. J., Weinshenker, D. and Swoap, S. J. (2007). Oxyntomodulin increases intrinsic heart rate in mice independent of the glucagon-like peptide-1 receptor. *Am. J. Physiol. Regul. Integr. Comp. Physiol.* **292**, R962-R970.
Starck, J. M. and Beese, K. (2001). Structural flexibility of the intestine of the Burmese python in response to feeding. *J. Exp. Biol.* **204**, 325-335.
Starck, J. M. and Beese, K. (2002). Structural flexibility of the small intestine and liver of garter snakes in response to feeding and fasting. *J. Exp. Biol.* **205**, 1377-1388.
Stevens, R. L., Colombo, M., Gonzales, J. J., Hollander, W. and Schmid, K. (1976). The glycosaminoglycans of the human artery and their changes in atherosclerosis. *J. Clin. Invest.* **58**, 470-481.
Van Mierop, L. H. S. and Kutsche, L. M. (1985). Some aspects of comparative anatomy of the heart. In: *Cardiovascular Shunts: Phylogenetic, Ontogenetic and Clinical Aspects* (ed. K. Johansen and W. W. Burggren), pp. 38-56. Copenhagen: Munksgaard.
Van Soldt, B. J., Danielsen, C. C. and Wang, T. (2015). The mechanical properties of the systemic and pulmonary arteries of *Python regius* correlate with blood pressures. *J. Morphol.* **276**, 1412-1421.
Wagenseil, J. E. and Mecham, R. P. (2009). Vascular extracellular matrix and arterial mechanics. *Physiol. Rev.* **89**, 957-989.
Wang, T., Taylor, E. W., Andrade, D. and Abe, A. S. (2001). Autonomic control of heart rate dring forced activity and digestion in the snake *Boa constrictor*. *J. Exp. Biol.* **204**, 3553-3560.
Wang, T., Zaar, M., Arvedsen, S., Vedel-Smith, C. and Overgaard, J. (2002). Effects of temperature on the metabolic response to feeding in *Python molurus*. *Comp. Biochem. Physiol. A* **133**, 519-527.
Wang, T., Altimiras, J., Klein, W. and Axelsson, A. (2003). Ventricular hemodynamics in *Python molurus*: separation of pulmonary and systemic pressures. *J. Exp. Biol.* **206**, 4241-4245.
Wearing, O. H., Conner, J., Nelson, D., Crossley, J. and Crossley, D. A., II (2017). Embryonic hypoxia programmes postprandial cardiovascular function in adult common snapping turtle (*Chelydra serpentina*). *J. Exp. Biol.* **220**, 2589-2597.
Woessner, J. F. (1976). Determination of hydroxyproline in connective tissues. In *The Methodology of Connective Tissue Research* (ed. H. A. Hall), pp. 227-233. Oxford: Joynson-Bruvvers Ltd.
Wolinsky, H. and Glagov, S. (1964). Structural basis for the static mechanical properties of the aortic media. *Circ. Res.* **14**, 400-413.
Zerbe, P., Glaus, T., Clauss, M., Hatt, J.-M. and Steinmetz, H. W. (2011). Ultrasonographic evaluation of postprandial heart variation in juvenile Paraguay anacondas (*Eunectes notaeus*). *Am. J. Vet. Res.* **72**, 1253-1258.